Micro Laser Melting: Analyses of Current Potentials and Restrictions for the Additive Manufacturing of Micro Structures

(Current Potentials of Micro Laser Melting)
Authors:

J. Fischer*, M. Kniepkamp*, E. Abele*

*Institute of Production Management, Technology and Machine Tools (PTW), Technische Universität Darmstadt, Germany

REVIEWED

Abstract

Although there is a significant requirement for complex micro parts, current metal processing additive manufacturing techniques are limited in achievable part accuracy and geometric resolution. Due to the recently developed process of Micro Laser Melting (MLM) new potentials in micro manufacturing are realizable.
This paper gives an overview of the present potentials of MLM using 316L steel powder. While using powder material with a grain size of ≤ 5 µm this technique enables layer thicknesses from 5 to 7 µm. Due to the use of different exposure strategies and laser modes (pulsed and continuous radiation) high aspect ratios up to 260 could be realized with thin wall structures. Furthermore, the influence of laser mode and exposure sequence on the part density, surface quality and accuracy of lattice structures with a minimum wall thickness lower than 40 µm is analyzed.

Introduction

Additive Manufacturing (AM) or 3D printing encompasses all current known layer-wise fabrication techniques for rapid prototyping (RP) or rapid manufacturing (RM). The development of these processes started around 1990 (Kruth, 1991). Due to the adding up of discrete layers, a high degree of design freedom for the manufacturing of complex parts is possible. The typical process advantages are near net-shape manufacturing, the possibility to realize a part direct from its CAD data and that no part geometry or feature specific tools are required. By selective laser melting (SLM) the repetitive melting and solidification of metal powder layers enables the creation of parts with similar mechanical properties like parts made to those of bulk material (Kruth *et al.*, 2005). This enables AM for the fabrication of parts for applications like automotive, aerospace and the medical industry. Due to trends like mass customization and the need of a higher functional integration AM is becoming an increasingly cost efficient possibility for the manufacturing of small to medium lot sizes. At the current state of SLM various metals (e.g. titanium (Over, 2003), (Osakada and Shiomi, 2006); aluminum (Zhang, 2004); various steels (Rombouts *et al.*, 2006) or its alloys are used.

In response to the miniaturization trend and the increasing of the micro production market the AM process had to be enhanced to fulfill such needs as achievable accuracy and resolution. In 2003 Regenfuss et al (Regenfuss *et al.*, 2005) presented microlaser sintering (MLS) or laser micro sintering as a newly developed approach of the selective laser sintering (SLS) process. At this time, the process showed the new potential to realize metallic parts smaller than 100 µm. Since then, different investigations were carried out to generate micro parts by using layer thicknesses lower than 10 µm and powder particle sizes smaller than $d_{50} = 5$ µm. Currently, different names, similar to the diverse terms for SLM, for MLS are common. The following Table 1 gives an overview of the current state:

Table 1: comparison of different investigations of additive metal manufacturing in the micro scale

	LHM, Mittweida	LZH, Hannover	ILT, Aachen
e.g. publications	(Regenfuß *et al.*, 2003; Regenfuß *et al.*, 2007; Exner *et al.*, 2008)	(Gieseke *et al.*, 2012b; Gieseke *et al.*, 2012a)	(Schniedenharn *et al;* Meiners, 2014)
processed Material	Tungsten, aluminium, copper, silver, 316L, molybdenum, titanium, 80Ni20Cr	316L	316L, nickel, H11 (1.2343)
Particle size	0.3 – 10 µm	5 – 25 µm	d_{50}= 7.9 µm
Focus diameter	25 µm	19.4 µm	30 µm
Laser power	0.5 – 2 kW	25 W	n.s.
Laser mode	pulsed 5 -20 kHz	continuous wave	continuous wave / pulsed
Layer thickness	n.s.	20-30 µm	10 µm
Achieved density	> 95%	n.s.	n.s.
Achieved aspect ratio	300 (10 µm notch)	30	n.s.
Smallest structure	ligaments 20 µm, notches 10 µm	30 µm thick wall	55 µm with cw 42.7 µm with pulsed mode
Surface quality	Ra = 1.5 µm	Ra = 8 µm	Ra = 1.47 µm Sa = 1 – 2 µm

In summary all these shown investigations follow the approach of increasing the resolution of the previously known SLM or SLS process which can be described as scalable techniques (Vaezi *et al.*, 2013). The described increase in resolution is realized by downscaling the significant size affecting parameters e.g. spot diameter, layer thickness and particle size. Although there are some more investigations about AM in the micro scale the followingdefinition for micro AM of (Gebhardt, 2013) which means that the typical dimensions of a manufactured part is in the range of 10 till 100 µm will be used. Typical for micro manufacturing with AM are scales like powder grain sizes lower than 10 µm, layer thicknesses under 10 µm and laser focus diameter smaller than 40 µm. With the ability to fit this definition for the micro additive manufacturing the Institute of Production Management, Technology and Machine Tools (PTW), TU Darmstadt shows in this paper the current potential of micro selective laser melting (µSLM) by processing the stainless steel 316L with a commercially available system from 3D-Microprint GmbH Chemnitz.

Experimental Setup

The processed material was gas atomized 316L, a material which was also used in micro AM (Table 1) and in different SLM studies (Kamath *et al.*, 2014b). The powder had a grain size of d_{50} = 3.5 µm and spherical particle shape (Figure 1). This material was also used for the base plate in the process.

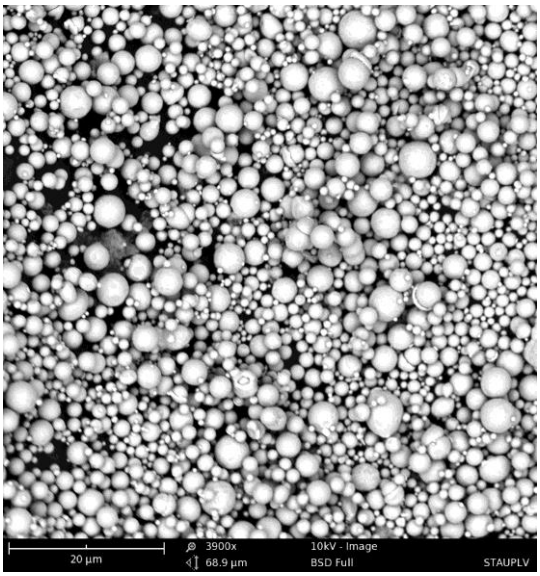

Figure 1: SEM of the used 316L stainless steel powder

For the investigations presented in this paper, an EOSINT µ60 micro laser sintering (MLS) system from 3D-Microprint GmbH Chemnitz was used. With this system it is possible to expose the powder layers in continuous and/or in Q-switch pulsed laser mode. The relevant system characteristics are shown in Table 2.

Table 2: Characteristics of the used AM system EOSINT µ60

laser power	30 W
focus diameter	30 µm
pulsed mode PRF	1 kHz - 1 MHz
scan speed	max 7 m/s
shielding gas	argon; O_2 & H_2O < 10 ppm
build envelope	max. Ø 56 mm * 30 mm

Experimental procedure

As described above continuous and pulsed laser exposition is commonly used for SLM in the micro scale (Regenfuß *et al.*, 2007), (Nölke *et al.*), (Schniedenharn *et al.*). Therefore a comparison of both exposure strategies at different process parameter settings is presented.

To identify stable process parameter combinations with the focus on the melt pool stability single track experiments were carried out. Previous experiments had shown, that due to the mean powder particle size of d_{50} = 3.5 µm a layer thickness of 7 µm leads to stable recoating results. As base plate material also 316L was used. To show the potentials of different laser modes for the manufacturing of micro parts, the continuous wave (cw) exposure was compared to the exposure using pulsed laser mode. The investigated process parameters for the single track experiments using continuous wave exposure were the scan speed (v_s), ranging from 100 mm/s to 3900 mm/s in steps of 200 mm/s, and the laser power (P_L), ranging from 1.5 W up to 30 W in steps of 1.5 W.

For the pulsed laser mode exposure single track experiments the pulse repetition rates (PRF) ranging from 10 kHz to 390 kHz steps of 20 kHz and the pulse distances (p_d) ranging 5 µm to

15 µm in 5 µm steps were additionally investigated. The pulse shape was kept constant as a ramp shapeand the pulse duration time was kept constant at 250 ns.

The single track experiments for both laser modes were repeated five times and the resulting single tracks were optically analyzed with a measurement microscope LEICA DM6000 at a magnification of 100X. After the track analysis a selection of the process parameters which are showing a stable melt pool behavior were selected. From these selected parameters the line energy levels (E_L) can be calculated using formula (1)

$$E_L = \frac{P_L}{v_s} \tag{1}$$

Based on the calculated line energy levels, parameter combinations with the highest, medium and lowest laser power were determined for the further density analyses.

For density analyses three cuboids with the dimension of 5 * 5 *6 mm³ for each parameter combination were generated. These cuboids were produced as multilayered solid test specimens for density measurements with a layer thickness of 7 µm. The hatching was carried out as a meander hatch strategy with a hatch space of h_s = 21 µm. This value for hatch space was used in relation to the suggestion of Meiners (Meiners, 1999), who prefers to set the hatch space as a factor of the laser focus diameter (f_d) times the hatch space factor. According his experiments a value of 0.7 is a good fit for selective laser melting of metal materials. The following the formula (2) can be used to calculate a value for h_s.

$$h_s = f_d * 0.7 \tag{2}$$

the angle increment between each layer was fixed to 83°. For this analysis three numbered cuboids per parameter setup were built. Each cuboid was placed by randomizing its position and its sequence of the parameter setup on the base plate. The position of the specimens occurred in a diagonal orientation to avoid an overlapping by the coating process.

During this and all other experiments, the oxygen and humidity level of the process chamber atmosphere was below 3 ppm. For the density measurement the separation of the probes from the base plate was done with a band saw at low cutting speeds. After the separation each specimen was cleaned with a cleaning procedure of the test specimens similar to (Kamath *et al.*, 2014a). All cuboids were separated and the three ones with the same process parameter setup were stored together in one beaker glass. The cuboids were cleaned in an ultrasonic bath in three steps, each took about 5 minutes. First a 5% solution of Sonoswiss Cleaner T4 SW-C T4 and deionized water was used, in the second step the probes were purged in pure deionized water. As a last cleaning step the cuboids were rinsed in technical pure isopropanol. For outgassing the probes were stored over the night and additionally dried for 90 minutes in a drying cabinet at 150° C with air circulation. The measurement of the density was done in relation to the suggested approach of Spierings and Levy (Spierings *et al.*, 2011) by using the Archimedes method. The density was calculated with the formula (3)

$$\rho_p = \frac{m_a}{m_a - m_{fl}} * \rho_{fl} \tag{3}$$

The total mass (m_a) at air of all three cleaned, dried and outgassed specimens for each parameter setup was measured together. For the weight measurement a calibrated Kern ABT 220-4M scale was used. After all specimens where measured dry, the mass (m_{fl}) in acetone of technical pureness was balanced. The temperature specific density ($\rho_{fl}(t)$) of acetone was used for the calculation of the part density (ρ_p) and so the formula (4) could be specified as

$$\rho_p = \frac{m_a}{m_a - m_{fl}} * \rho_{fl}(t) \tag{4}$$

To indicate the achievable aspect ratio a lattice structures in a single track layout for each wall with different line energy levels were build. The distance from wall to wall was 500 µm, the dimension in the x-y-plane 5 * 5 mm² and the height 15 mm. The wall thickness of each specimen structure was measured on 50 different points along the walls with a LEICA DM 6000 microscope at a magnification of 100X and a resolution of 0.5µm.

To analyze the possible surface quality the parameter combination which achieved the highest density levels was used to build a test specimen which had the dimensions of 20 * 20 * 1 mm³. The exposure strategy was the same as in the density analyses. According to (DIN EN ISO 4288) three measurements of a length of 17.5 mm were taken in three different orientations to the build direction of the specimen. To quantify the achievable surface quality the value of the arithmetical mean roughness R_a was determined by the use of a MarSurf GD25 and a MFW-250 tracing arm from Mahr GmbH Germany.

Results and Discussion

Single track experiments

Based on the results of the single track analyses all experiments for continuous wave and pulsed laser mode were categorized into the occurred phenomena.

The melt pool stability shows six different levels of process stability in the single track experiments within the continuous wave laser mode exposure. These six levels are reaching from not visible tracks over occurred balling phenomena, tracks with defects or inhomogeneity to tracks which were homogeneous. The resulting process stability chart is shown in Figure 2.

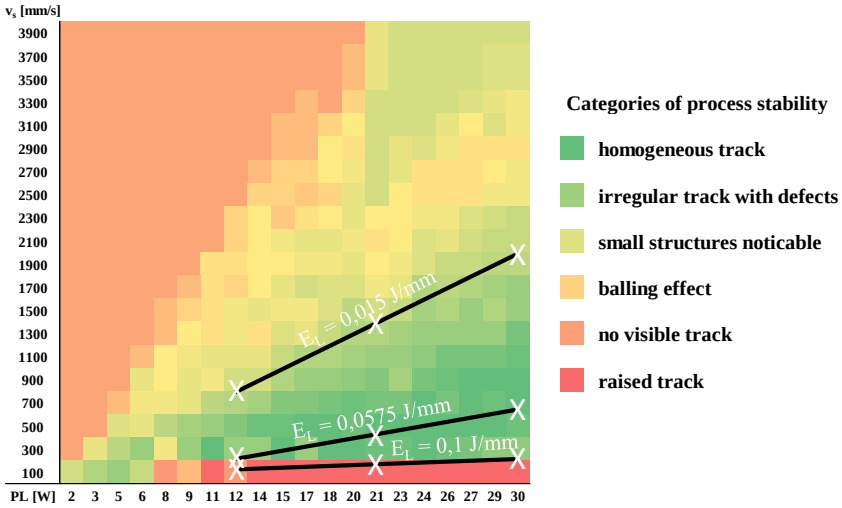

Figure 2: process stability chart during the single track experiments with cw exposure and a variation of laser power and the scan speed

The raised track phenomena which occurred at line energies higher than E_L = 0.1 J/mm results in tracks where fragments of the track are higher than the actual layer thickness. At line energy levels below E_L = 0.1 J/mm, tracks with a homogeneous width and shape with no partial molten powder particles at the track itself can be determined. These smooth and steady tracks occur between a line energy density of E_L = 0.1 J/mm and around E_L = 0.6 J/mm. With a decrease of the line energy under a level of E_L = 0.015 J/mm the number of defects on the

tracks is increaing significantly. With a further decrease of the line energy level, only some small fragments or ruins can be identified. Due to higher scan speeds, the balling effect also occurs. At line energy levels below $E_L = 0.006$ J/mm no melt pool or visible track can be recognized. In Figure 3 an overview of the occurred phenomena's and the categorization of these are shown.

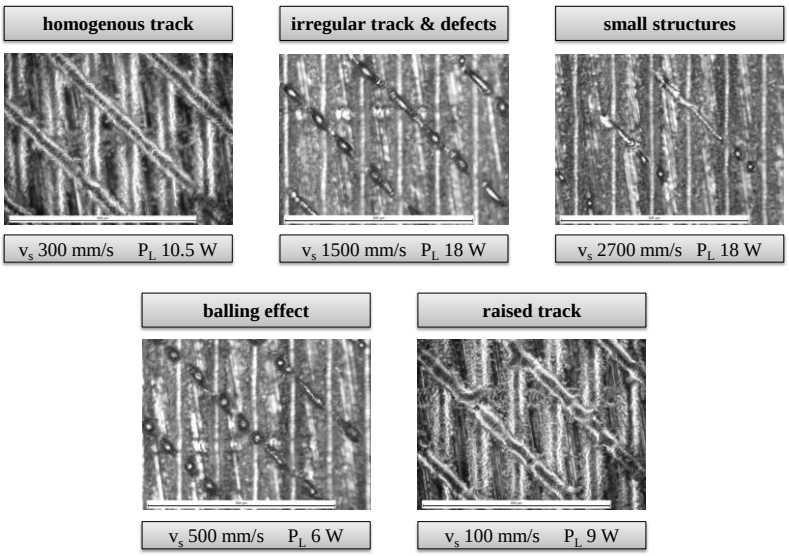

Figure 3: microscope visions (100X) of the described categories during the single track experiments with continuous wave laser mode exposure

To analyze the melt pool stability using the pulsed laser mode, an influence of pulse distance which was varied from $p_d = 5$ µm up to $p_d = 15$ µm can be determined. In the experiments with $p_d = 5$ µm mainly irregular tracks or sublimation of the base plate material occurs. The sublimation of base plate material means that material is removed due to excessively high energy input into the base plate by the pulsed laser energy. As an effect of this the base plate is irregularly engraved along the track path.

With an increase of the pulse distance at most combinations no visible track can be recognized. Especially with a pulse distance of $p_d = 15$ µm no visible structure of a melt pool or of the scanned track is recognizable. At a pulse distance of $p_d = 10$ µm an area of irregular tracks with defects and also balling occurs between both the other phenomena of sublimation and no visible structure. In Figure 4 the process chart of the pulsed exposure analyses is shown.

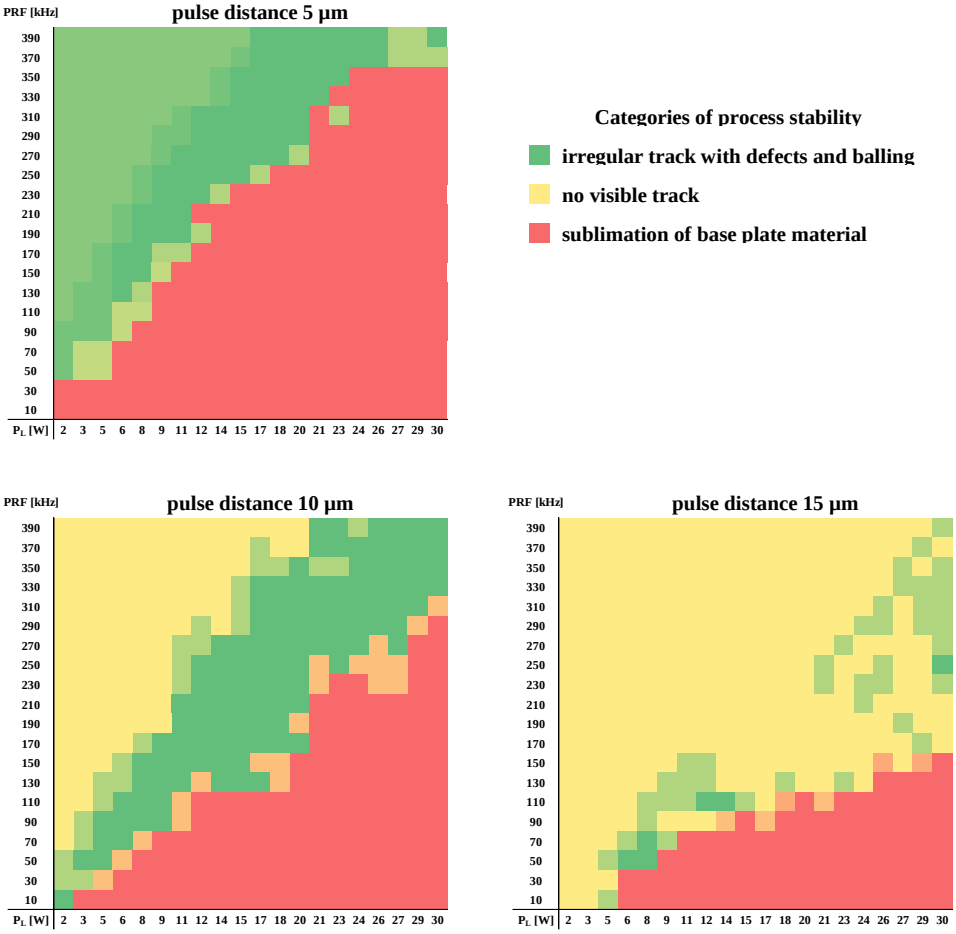

Figure 4: process stability chart stability during the single track experiments with a variation of laser power, pulse repetition rate and the pulse distance during pulsed laser exposure

Overall experiments no stable melt pool can be achieved, so that no process parameter combination for a homogenous track can be determined. Figure 6 gives examples for the different phenomena occurring in the pulsed mode exposure.

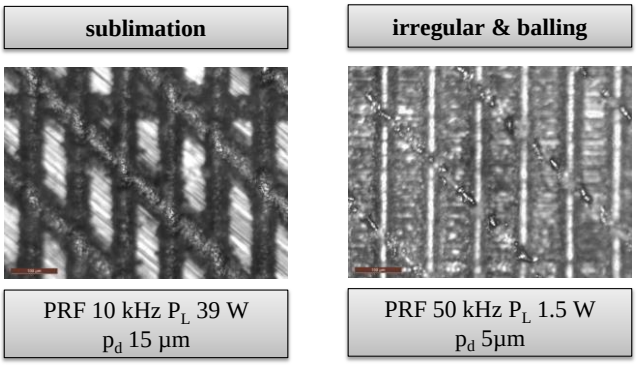

Figure 5: microscope visions (100X) of the described categories during the single track experiments with pulsed laser mode exposure

The pulsed laser mode tracks cannot be compared with the achieved process stability of the continuous wave laser mode generated tracks. All the so-called irregular tracks have a high number of defects and occurred high rate of balling can be seen. Due to this poor process

stability at the analyzed single pulsed exposure, no further analyses were carried out with pulsed laser mode exposure.

Density analyses: variation of line energy level EL

For the further investigations, a first setup of process parameters (black lined area in Figure 3) were used to analyze the influence of the line energy level to the track width. The used parameter combinations of the laser power and the scan speed were estimated by the use of formula 1. The observed line energy levels which were used to calculate these combinations were the lower (E_L = 0.015 J/mm) and the higher line energy level (E_L = 0.1 J/mm) of the area of a stable melt pool behavior shown in Figure 3. Also the medium line energy level of E_L = 0.015 J/mm was used to analyze the achievable track width. The determined parameter combinations are shown in Table 3.

Table 3: Process parameter setups for density analyses

Process parameter #	laser power P_L [W]	scan speed v_s [mm/s]	line energy [J/mm]
1	12	800	0.015
2	21	1400	
3	30	2000	
4	12	210	0.0575
5	21	370	
6	30	520	
7	12	120	0.1
8	21	210	
9	30	300	

The resulting track width due to the use of these parameter combinations is in the range of 23 µm and 69 µm. A microscope image and the measured track width w_{track} value, which was measured ten times, for each parameter combination is shown in Figure 6.

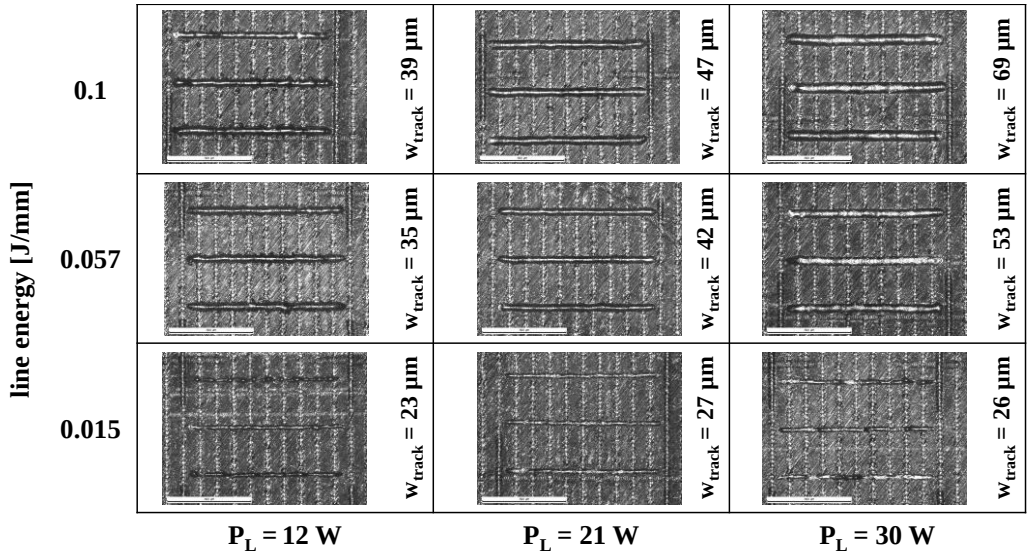

Figure 6: track width of the different parameter setups at the single track experiments with continuous wave exposure

With the in Table 3 shown parameter setups and a constant hatch space of h_s = 21 µm multilayered cuboids for the density analyze were generated. In this experiment high levels for the relative density up to ρ_{rel} = 99.31 % can be reached (Figure 7).

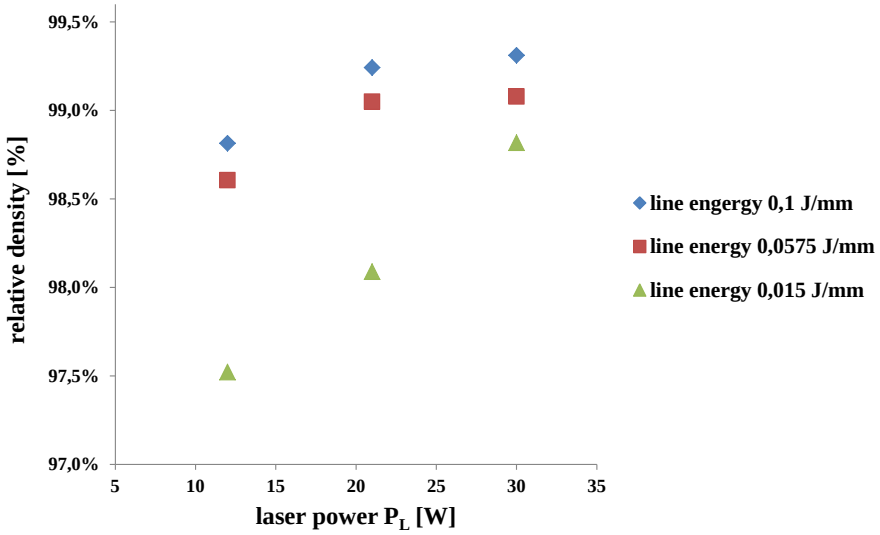

Figure 7: influence of the line energy to the achievable relative density with continuous waver exposure

At higher line energy levels of E_L = 0.0575 J/mm and E_L = 0.1 J/mm, an increase in the laser power from P_L = 21 W up to P_L = 30 W, does not lead to a significant increase of the relative density.

At the lower line energy level of E_L = 0.015 J/mm the increase in the laser power has a significant influence to the density. The increase of the relative density is reaching a value of $\Delta\rho_{rel}$ = 1.3 % for a laser power increase from P_L = 12 W to P_L = 30 W, which equates a ΔP_L = 18 W.

The parameter with the highest scan speed of v_s = 2000 mm/s and a laser power of p_L = 30 W results in an acceptable relative density of ρ_{rel} = 98.82 %. In relation this scan speed setup is around 6.6 times higher in compared to the scan speed parameter of v_s = 300 mm/s which results in a relative density of ρ_{rel} = 99.31 %. With an increase of the scan speed by the factor of 6.6 only a decrease $\Delta\rho_{rel}$ = 0.49 % occurs. This result shows that in a relatively wide range of line energy parts with a high relative density can be realized by µSLM using continuous wave laser mode.

Density analyses: variation of hatch space hs

To analyze the impact of the hatch distance on the density the parameter combination which resulted in the highest density of ρ_{rel} = 99.31 % was used. At a laser power of P_L = 30 W and a scan speed of v_s = 300 mm/s, the hatch distance was varied between h_s = 14 µm and h_s = 45 µm in 6 µm steps. The results of the density analyses can be seen in figure 8.

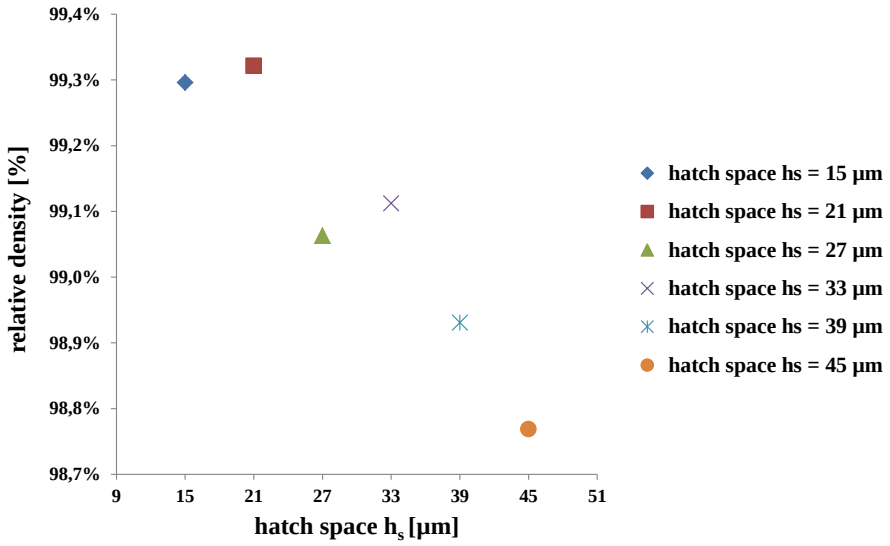

Figure 8: influence of the hatch space to the achievable relative density with continuous waver exposure at a laser power P_L = 30 W and a scan speed of v_s = 300 mm/s

The decrease of the hatch distance from h_s = 21 µm to h_s = 15 µm is resulting in a very small decrease of the relative density $\Delta\rho_{rel}$ = 0.02 %. With an increase of the hatch space the relative density is decreasing. The density decrease reaches a value of $\Delta\rho_{rel}$ = 0.55 % while the hatch space was increased more than two times to a value of h_s = 45 µm.

In the single track experiments the parameter combination of a laser power P_L = 30 W and a scan speed of v_s = 300 mm/s results in a track width of w_{track} = 69 µm. It was to be expected that with an increase of track width the hatch space could be increased without a decrease in density. However the investigation shows a decrease in density due to higher hatch spaces.

This can be explained by the scan overlap of a single track at the low hatch distances when building with parallel tracks. In this context the in the first density analyses found parameter setup of a laser power of P_L = 30 W, a scan speed of v_s = 300 mm/s and a hatch space h_s = 21 µm giving again a good potential to achieve a high relative density.

Analyses of achievable aspect ratio

The lattice structures for the aspect ratio analyses were built using the three different line energy levels of the density investigations at the highest laser power of P_L = 30 W. It was not possible to build a lattice structure using the lowest line energy of E_L = 0.015 J/mm. Only two lattice structures can be analyzed. The measured wall thickness and the achieved aspect ratio at the height of 15 mm can be seen in Figure 9.

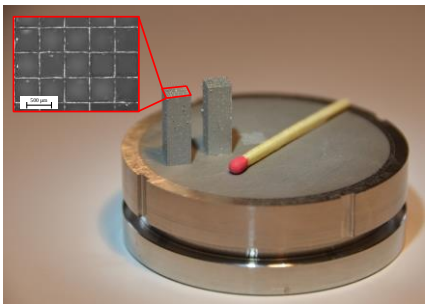

	wall thickness	aspect ratio
E_L = 0.1 J/mm	73 µm	204
E_L = 0.0575 J/mm	57 µm	262
E_L = 0.015 J/mm	No lattice structure built	

Figure 9: results of the aspect ratio analyzes

This result shows, that a low line energy level of E_L = 0.015 J/mm can be used to create cuboids with a high density but is not possible to build thin wall lattice structures with it. Compared to the single line experiments the wall thickness is increasing minimal by adding up layers to a structure.

Analyses of surface quality

The orientation of the analyzed planes and the measured arithmetical mean roughness Ra is shown in Figure 10.

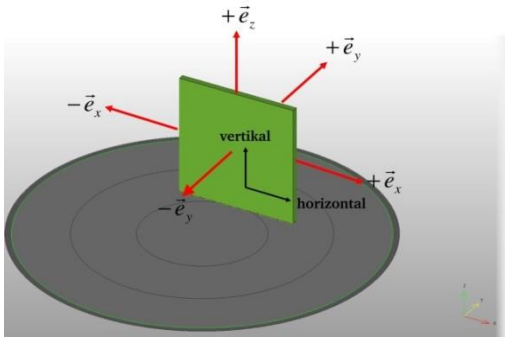

	Ra_{mean}
- ex – $plane_{vertical}$	8.00 µm
- e_y – $plane_{horizontal}$	8.38 µm
- e_y – $plane_{vertical}$	9.43 µm
+ e_z – plane	7.29 µm

Figure 10: surface measurement at the tested wall and Ra_{mean} values at the different surfaces

The best surface quality can be achieved on the top face (+ e_z – plane) with Ra_{mean} = 7.29 µm. These results confirm influence of the orientation of surfaces to the build direction on the surface quality. Caused by partly molten powder particles the quality of vertical orientated surfaces is not as good as the surface quality of horizontal orientated ones. The relatively high surface roughness values in relation to the used powder particle size can be explained with the used exposure strategy. Due to the rotation of the scan vectors most of the vectors are not parallel to the outer surfaces of the part, resulting in higher surface roughness. An additional contour scan could be used to obtain higher surface qualities. This will be the focus in future studies.

Summary

In the presented paper, the current potentials of µSLM using 316L are shown. The exposure of continuous wave laser mode and pulsed laser mode were compared and, due to the instability of the single track at pulsed laser mode, only continuous wave laser mode was investigated in further experiments, which focused on the achievable density, surface quality and aspect ratio. Using continuous wave laser mode exposure, it is possible to reach the following characteristics:

- a relative density of ρ_{rel} = 99.32 %
- a medium influence of the line energy level at low laser power levels was shown
- an increase of the scan speed by the factor of 6.6 leads only to a decrease of the relative density $\Delta\rho_{rel}$ = 0.49 %
- a small influence of the hatch space between the shown parameters consists, this may be used to increase the building rate
- surface qualities between arithmetical mean roughness Ra = 7.29 – 9.43 µm
- aspect ratios up to 262 with single standing thin walls can be realized

Furthermore with the pulsed laser mode using a single exposure strategy, only a poor single track quality in comparison to the continuous wave laser mode occurred. In further investigations, the pulse mode will be focused on to identify its potential in comparison to that which has been demonstrated in the work of other researchers.

Acknowledgment

The presented results were supported by the LOEWE Research Center AdRIA (Adaptronics – Research. Innovation. Application). The authors would like to thank the German research Foundation (DFG) and the Hessian State Ministry of Higher Education, Research and the Arts for the funding which enabled the presented results.

References

Deutsches Institut für Normung (1998), *Geometrische Produktspezifikation (GPS) - Oberflächenbeschaffenheit: Tastschnittverfahren - Regeln und Verfahren für die Beurteilung der Oberflächenbeschaffenheit*, ICS 17.040.20 DIN EN ISO 4288, Beuth Verlag, Berlin.

Exner, H., Horn, M., Streek, A., Ullmann, F., Hartwig, L., Regenfuß, P. and Ebert, R. (2008), "Laser micro sintering: A new method to generate metal and ceramic parts of high resolution with sub-micrometer powder", *Virtual and Physical Prototyping*, Vol. 3 No. 1, pp. 3–11.

Gebhardt, A. (2013), "Generative Fertigungsverfahren. Additive manufacturing und 3D-Drucken für Prototyping - Tooling - Produktion", *Generative Fertigungsverfahren*.

Gieseke, M., Kirbach, S., Hustedt, M., Kaierle, S., Wesling, V. and Haferkamp, H. (2012a), "Additive Fertigung komplexer Mikroimplantate", *Mikroproduktion No.* 1, pp. 26–31.

Gieseke, M., Senz, V., Vehse, M., Fiedler, S., Irsig, R., Hustedt, M., Sternberg, K., Nölke, C., Kaierle, S., Wesling, V., Tiggesbäumker, J., Meiwes-Broer, K.-H., Seitz, H., Schmitz, K.-P. and Haferkamp, H. (2012b), "Additive Manufacturing of Drug Delivery Systems", *Biomedical Engineering / Biomedizinische Technik*, Vol. 57 SI-1 Track-S.

Kamath, C., El-dasher, B., Gallegos, G.F., King, W.E. and Sisto, A. (2014a), "Density of additively-manufactured, 316L SS parts using laser powder-bed fusion at powers up to 400 W", *The International Journal of Advanced Manufacturing Technology*.

Kamath, C., El-dasher, B., Gallegos, G.F., King, W.E. and Sisto, A. (2014b), "Density of additively-manufactured, 316L SS parts using laser powder-bed fusion at powers up to 400 W", *The International Journal of Advanced Manufacturing Technology*.

Kruth, J.P. (1991), "Material Incress Manufacturing by Rapid Prototyping Techniques", *CIRP Annals - Manufacturing Technology*, Vol. 40 No. 2, pp. 603–614.

Kruth, J.P., Vandenbroucke, B., Vaerenbergh, Ing. J. van and Mercelis, P. (Eds.) (2005), *Benchmarking of different SLS/SLM processes as Rapid Manufacturing techniques*, Gent, Belgium.

Meiners, W. (1999), *Direktes selektives Laser-Sintern einkomponentiger metallischer Werkstoffe, Berichte aus der Lasertechnik*, Als Ms. gedr., Shaker, Aachen.

Meiners, W. (2014), *Abschlussbericht MikroGen: Entwicklung, Erprobung und Systemintegration hochpräziser, generativer Laserverfahren in der industriellen Fertigung*.

Nölke, C., Gieseke, M. and Kaierle, S., "Additive manufacturing in micro scale", October 6 - 10, 2013, Hyatt Regency, Miami, Florida, USA.

Osakada, K. and Shiomi, M. (2006), "Flexible manufacturing of metallic products by selective laser melting of powder", *International Journal of Machine Tools and Manufacture*, Vol. 46 No. 11, pp. 1188–1193.

Over, C. (2003), *Generative Fertigung von Bauteilen aus Werkzeugstahl X38CrMoV5-1 und Titan TiAl6V4 mit "Selective Laser Melting", Berichte aus der Lasertechnik*, Shaker, Aachen.

Regenfuß, P., Ebert, R. and Exner, H. (2007), "Laser Micro Sintering – a Versatile Instrument for the Generation of Microparts", *Laser Technik Journal*, Vol. 4 No. 1, pp. 26–31.

Regenfuss, P., Hartwig, L., Klötzer, S., Ebert, R., Brabant, T., Petsch, T. and Exner, H. (2005), "Industrial freeform generation of microtools by laser micro sintering", *Rapid Prototyping Journal*, Vol. 11 No. 1, pp. 18–25.

Regenfuß, P., Hartwig, L., Klötzer, S., Ebert, R. and Exner, H. (2003), "Microparts by a Novel Modification of Selective Laser Sintering", 12.-15.5.2003, Chicago, Illinois, USA.

Rombouts, M., Kruth, J.P., Froyen, L. and Mercelis, P. (2006), "Fundamentals of Selective Laser Melting of alloyed steel powders", *CIRP Annals - Manufacturing Technology*, Vol. 55 No. 1, pp. 187–192.

Schniedenharn, M, Belting, Batista, S., J, R., Meiners, W and Weisheit, A., “Micro scale laser based additive manufacturing for metals”, October 6 - 10, 2013, Hyatt Regency, Miami, Florida, USA.

Spierings, A., Schneider, M. and Eggenberger, R. (2011), “Comparison of density measurement techniques for additive manufactured metallic parts”, *Rapid Prototyping Journal*, Vol. 17 No. 5, pp. 380–386.

Vaezi, M., Seitz, H. and Yang, S. (2013), “A review on 3D micro-additive manufacturing technologies”, *The International Journal of Advanced Manufacturing Technology*, Vol. 67 5-8, pp. 1721–1754.

Zhang, D. (2004), *Entwicklung des Selective Laser Melting (SLM) für Aluminiumwerkstoffe, Berichte aus der Lasertechnik*, Shaker, Aachen.